BEAM COMPRESSION IN HEAVY-ION INDUCTION LINACS*

P.A. Seidl[1#], A. Anders[1], F.M. Bieniosek[1], J.J. Barnard[2], J. Calanog[1],3, A.X. Chen[1,3], R.H. Cohen[2], J.E. Coleman[1,3], M. Dorf[4], E.P. Gilson[4], D.P. Grote[2], J.Y. Jung[1], M. Leitner[1], S.M. Lidia[1], B.G. Logan[1], P. Ni[1], P.K. Roy[1], K. Van den Bogert[1], W.L. Waldron[1], D.R. Welch[5],
[1]Lawrence Berkeley National Laboratory, Berkeley, CA 94720, USA
[2]Lawrence Livermore National laboratory, Livermore, CA 94550, USA
[3]University of California, Berkeley, CA 94720, USA
[4]Princeton Plasma Physics Laboratory, Princeton, NJ 08543-0451, USA
[5]Voss Scientific, Albuquerque, NM 87108, USA

Abstract

The Heavy-Ion Fusion Sciences Virtual National Laboratory is pursuing an approach to target heating experiments in the Warm Dense Matter regime, using space-charge-dominated ion beams that are simultaneously longitudinally bunched and transversely focused. Longitudinal beam compression by large factors has been demonstrated in the LBNL Neutralized Drift Compression Experiment (NDCX) experiment with controlled ramps and forced neutralization. The achieved peak beam current and energy can be used in experiments to heat targets and create warm dense matter. Using an injected 30 mA K^+ ion beam with initial kinetic energy 0.3 MeV, axial compression leading to ≈50x current amplification and simultaneous radial focusing to beam radii of a few mm have led to encouraging energy deposition approaching the intensities required for eV-range target heating experiments. We discuss experiments that are under development to reach the necessary higher beam intensities and the associated beam diagnostics.

INTRODUCTION

To create a short (~ ns) pulse with duration suitable for the study of warm dense matter [1], our approach has been to modulate the energy of an initially much-longer non-relativistic beam. To achieve target temperatures around ~ 1 eV, the required beam intensity calls for space charge neutralization, which has been achieved with a background plasma through which the beam passes while it is focusing transversely and bunching longitudinally.

We are approaching the required beam intensities for heating targets toward warm dense matter conditions, and have arrived at this stage through a sequence of experiments over the past several years. The scaled final focusing experiment demonstrated the successful neutralization of an initially space-charge-dominated beam by a background source of electrons in order to achieve an emittance-limited focal spot [2]. The experiment was scaled from a design of a final focusing system for a heavy ion fusion driver using quadrupole magnets for beam transport (driver parameters: 10 GeV Bi^+ at 1.25 kA/beam). Following initial experiments with an emittance-limited 95 μA, 160 keV Cs^+ beam, the beam current was then increased to 400 μA with a perveance of 5 x 10^{-5}; space-charge limited near the focal plane for an un-neutralized beam. The spot radius with neutralization was ~2X smaller, in agreement with models assuming 80% and 0% neutralization, respectively. LSP simulations [3] showed good agreement with the experiments.

Next, the Neutralized Transport Experiment, used a higher current (~25 mA) and higher energy (250-350 keV) K^+ beam. The beam perveance (~10^{-3}) was effectively neutralized with RF and cathodic-arc plasma sources [4]. This demonstrated the feasibility of neutralization of higher perveance beams, a precursor to the additional feature of axial bunching of the ion beam.

The axial compression is achieved with an induction bunching module (IBM) inserted after the matching section. Operating at ±80 kV, a ±12.5% velocity ramp is imparted to 150-200 ns subset of the several-microsecond beam pulse. The beam then drifts through a neutralizing plasma in a drift compression section a few meters in length (L). To establish a neutralizing plasma along most of the length of the drift compression section, the RF plasma used in NTX was replaced with a ferro-electric plasma source [5], and cathodic arc plasma sources injected a high-density plasma near the focal plane where the beam density is greatest. Current amplification of ≈ 50 was demonstrated in the first NDCX experiments [6].

A fundamental limit to the current amplification and pulse duration is the longitudinal energy spread (longitudinal phase space and emittance) of the injected beam, as shown in Eq. 1:

$$t_{\min} = \frac{L}{v^2}\sqrt{\frac{2kT}{M}} \qquad (1)$$

where v is the average ion velocity, T is the effective longitudinal beam temperature and M is the ion mass.

The energy spread was measured with an electrostatic energy analyzer. The measured energy spread is adequate for achieving nanosecond-duration bunches (see below). Other limits are set by the uniformity and density of the background neutralizing plasma, and imperfections of the bunching module waveform. In general, simulations have shown that if the background plasma density is greater than the local beam density, then the effectiveness of the neutralization is independent of the details of the plasma density distribution [7]. For near-term warm dense matter experiments, the beam density increases steeply and

* This work supported by the U.S. Dept. of Energy contracts W-7405-ENG-48, DE-AC02-05CH11231 and DE-AC02-76CH-O3073.
#PASeidl@lbl.gov

approaches $n_b = 10^{13}$ cm^{-3} near the target plane. We have measured plasma densities in that range with cathodic-arc plasma sources. The plasma temperature should be low enough to not heat the beam and we have found that plasma temperatures in the few eV range have a benign influence on the beam. Depending on the beam and plasma densities, collective instabilities may limit the focused beam intensity, but for NDCX-I (based on both experiment and theory) and NDCX-II (based on theory) these instabilities appear to be benign.

RESULTS AND DISCUSSION

We installed a short, high-field solenoid (B = 8 Tesla, 10-cm coil length) after the ferroelectric plasma source and before the target plane (Fig. 1) to impart a steep convergence angle on the beam before the focal plane. LSP modeling suggests that sub-mm radii might be possible, leading to a several-fold increase in the energy deposition. This assumes sufficiently high plasma density can be injected into the bore of the solenoid [8]. A target chamber and new target heating diagnostics have been installed at the end of the beamline [9].

Beam Diagnostics in the Target Chamber

An improved Fast Faraday Cup has been installed in the new target chamber (See Fig. 1). The operating principle is the same as in ref. [10] and the electronic response still allows for ≈1 ns resolution of the ion beam current. This is established mainly by the 1-mm gap between the suppressor plate and the collector, since the incoming ion (v ≈ 1.2 m/μs) transit time of 1 ns will set the scale for the capacitive pickup of the ions approaching the collector. The new design enables variation of gaps between hole plates, and hole plate transparency, easier alignment of the front hole plate to middle (bias) hole plate, and a metal enclosure for shielding from the background plasma and electronic noise. Each hole plate has a hexagonal array of holes, extending over a circular area with 30-mm diameter. In the current version, the front hole plate (held at ground potential) has 0.23 mm diameter holes spaced by 1 mm, while the middle hole plate (suppressor grid, biased to -75 V) has 0.46 mm diameter holes spaced by 1 mm. The holes are larger on the middle plate to prevent scraping. This 95-mrad tolerance between the concentric front plate holes and the middle plate holes should compensate for non-zero ion trajectories and detector alignment imperfections. The collector plate is biased to +75 V.

The geometric transparency of the front hole plate results in a reduction of the beam current reaching the collector grid by a factor of 44. Figure 2 shows the response of the Faraday cup to the uncompressed head of the beam (30 mA K^+, 1 μs duration), and the compressed bunch at t ≈ 4.8 μs. The product of the collector signal amplitude and the hole plate transparency agrees (≈±5%) with the upstream measurement of the beam current before the IBM. The suppressor signal has a similar response to the collector, and is not as well understood at this time. We are modeling the detector response with WARP and LSP particle in cell simulations, including the effect of desorption and ionization of neutral atoms from the collector and front plate. The recognition of this latter effect as potentially significant is based on analytic estimates using known desorption coefficients, charge-exchange cross sections and ionization cross sections. We are also studying the possibility that ions are striking the middle plate due to detector misalignment, beam centroid misalignment, and large angle ion trajectories from the chromatic aberrations and also due to small angle scattering from the inside edge of the front plate holes.
Though simulations show that the collector should be effectively shielded from the plasma is by the front hole plate, a plasma background signal from the FCAPS has been measured on the collector. It is slowly varying and is subtracted during data analysis.

The transverse (spatial) distribution of the beam is measured by allowing the beam to strike a 100-micron thick alumina scintillator, and then detecting the beam induced light emission with an image-intensified gated-MCP camera. The optical system produced a resolution of 10 to 17 pixels/mm (depending on the choice of lens and

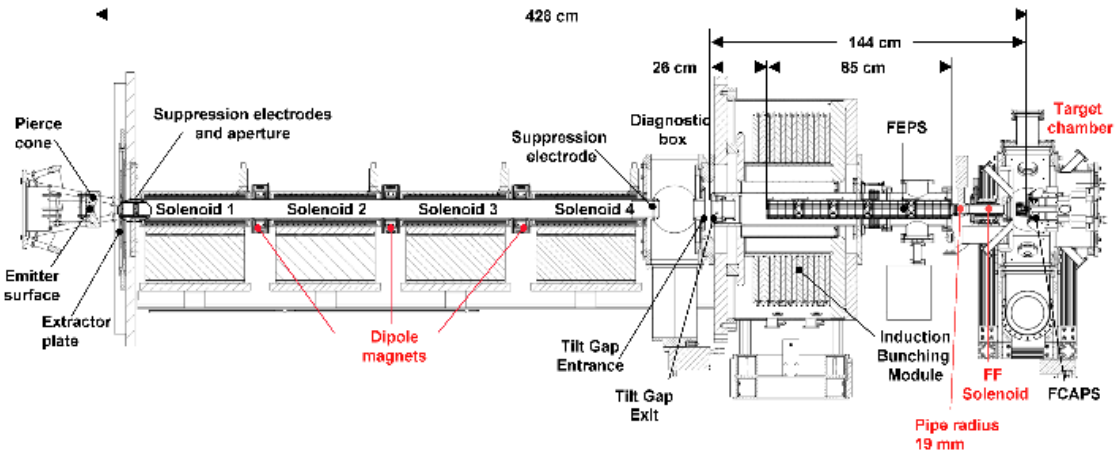

Figure 1: Elevation view of the Neutralized Drift Compression Experiment

optical setup). Image acquisition and processing software are then used to collect and analyze the time-gated images of the beam [11]. A steel mesh of transparency 28% is placed on the upstream side of the scintillator. The relatively low transparency reduces the flux onto the scintillator and the degradation of the scintillator. It is biased to -300 V, creating a supply of electrons to discharge the scintillator caused by the accumulation of charge from the positive ion beam. Using a phototube, photodiode, and streak camera, the time dependence of the light output from the scintillator has been recorded to measure the compressed pulse duration independently of the fast Faraday cup.

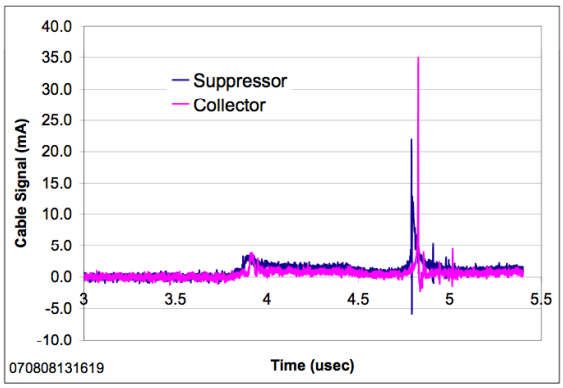

Figure 2: Faraday cup response to uncompressed beam and bunched portion ($t \approx 4.8$ μs).

Longitudinal Phase Space Measurements

The energy spread, ΔE, of the non-relativistic ion beam is related to the longitudinal velocity spread Δv_z by $\Delta E = mv\Delta v_z$. Assuming the velocity distribution is a one-dimensional Maxwellian about the mean beam velocity, the temperature, T_z, of that distribution is given by:

$$T_z = \frac{(\Delta E^2)}{2E_o} \qquad (2)$$

The new electrostatic energy analyzer (EEA) was placed at the exit of the ferro-electric plasma source, to measure the longitudinal phase space and energy spread of the uncompressed beam with and without plasma neutralization [12, 13]. A special beam envelope tune was used for the un-neutralized beam to prevent particle loss in the 180-cm drift distance from the final matching solenoid to the entrance slit of the spectrometer. The entrance slit of the spectrometer was 0.1 mm x 5 mm, which allowed ~10 μA of the incident 30-mA K^+ beam to be transmitted through the spectrometer, a 90-degree sector design with a bending radius of 75 cm and a gap of 2.5 cm between concentric dipole electrodes. The focal plane detectors were a slit-Faraday cup and an alumina (Al_2O_3) scintillator with a gated CCD camera. For a 300 keV ion beam, deflection plate voltages were ±15 kV. The contribution of field quality to spectrometer resolution was estimated with ray tracing simulations with fields derived from the mechanical specifications of the field defining plates. The results suggest a resolution of $\Delta E/E \approx 5 \times 10^{-5}$, while the contribution from the 0.1 mm entrance slit gives a resolution of $\Delta E/E = 2 \times 10^{-4}$ or $\Delta E = 60$ eV. Thus, the choice of entrance slit width (motivated by detector signal-to-noise) is the dominant factor in determining the energy resolution for these data. The dispersion on the focal plane is 1.7 mm / keV and this is reflected in the data of Fig. 3, showing the profiles of a 500-ns slice of the 289 keV incident beam for several dipole plate voltages.

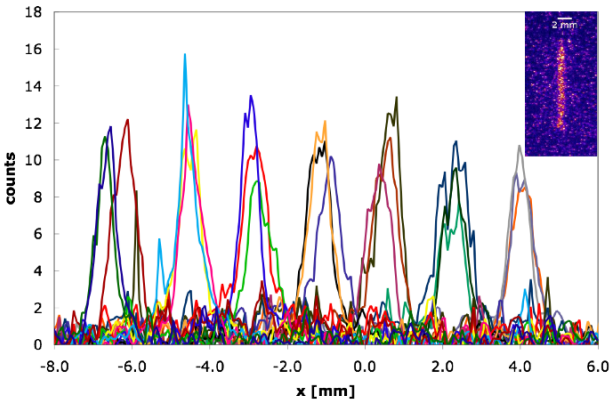

Figure 3: Beam image profiles as a function of deflection plate voltages. The incident beam energy was 289 keV, and the deflection plate voltages were scanned in 50-Volt steps around 14.5 kV, corresponding to beam energy variations of 1-keV steps. The inset shows one of the images from the scintillator (at $x \approx -1$ mm).

The data were measured with the scintillator and image-intensified CCD camera. The entire energy acceptance of the spectrometer is displayed, about 7 keV. The variation among repeated beam pulses (three per plate voltage setting) shows the shot-to-shot energy variation of the beam, <0.1 keV (rms). The measured width of the distributions, or the energy spread of the injected E_o = 289-keV un-bunched beam is $\Delta E \approx 0.17$ keV. The measured energy spread corresponds to an axial temperature of $T_z = 0.05$ eV, which is adequate for compressing the beam to < 1 ns (Eq. 1). Other mechanisms may limit the pulse duration, such as incomplete neutralization of the compressed pulse, and waveform imperfections in the IBM. No significant difference was observed between the neutralized and un-neutralized beam cases, suggesting minimal heating of the beam from the FEPS plasma.

The time dependence of the energy distribution was recorded with a streak camera imaging the light emission from the scintillator (Fig. 4), and independently with a slit-Faraday cup. The results reflect the slight decrease (2-4 kV/μs) of the injector Marx voltage after the initial rise to peak voltage. Signal to noise limitations obscured the detection of the acceleration of ions near the head of the beam due to longitudinal space charge. Particle-in-cell simulations suggested this would be a difficult signal to detect due to low signal amplitude.

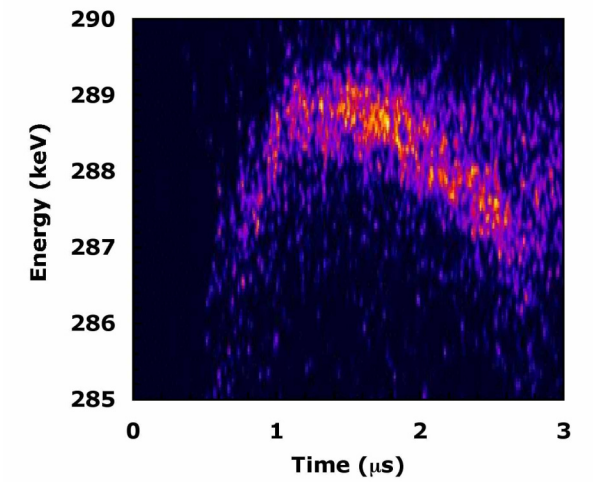

Figure 4: Streak camera image of the longitudinal phase space of the uncompressed beam near the beginning of the pulse.

Plasma Density Measurements

The plasma density in the target chamber has been increased and now mostly exceeds the on-axis beam density to satisfy $n_p/n_b>1$, where n_p and n_b are the plasma electron density and ion beam density, respectively, and Z is the mean ion charge state of the plasma ions. This work consists of several segments. First the plasma density of two filtered cathodic arc plasma sources (two-FCAPS) was measured with an axially moveable Langmuir probe with a 4-Tesla solenoid magnetic field. Next, the two-FCAPS system was replaced by fabricating four cathodic arc plasma sources (four-FCAPS) with straight filters (vs the former 45° bend in the two-FCAPS system) to increase the plasma density. The solenoid magnetic field was increased to 8 T. Results show that the new four-FCAPS system, with the short straight filters and driven with a 3x higher discharge current provides 9-60 times greater plasma density than the two-FCAPS system with the bent filters. Assuming a mean plasma velocity of $2x10^4$ m/s, the four-FCAPS system provided a peak plasma density 9 x 10^{12} – 6 x 10^{13} /cm^3. Finally, the axial and radial plasma distribution was measured with a specially designed array of 37 Langmuir probes. These new data shows that plasma forms a thin column of diameter ~5 mm along the solenoid axis when the Final Focus Solenoid (FFS) is energized. The results are described in [14].

Beam Compression and Focusing Results

A new 8-Tesla pulsed Final Focus Solenoid (FFS) has been fabricated and installed at the target chamber entrance, and replaces the prototype solenoid that produced a 5-Tesla peak field. The peak field of the first solenoid was limited by high-voltage flashover near the magnet leads and later was limited to 4 Tesla peak field. The mechanical design and cooling system of the solenoid were improved, and the new solenoid consistently operates up to the design value of 8 Tesla.

The Faraday cup in the Diagnostic box has been used to measure the beam current transported to the entrance of the IBM. This measurement is used in a cross-normalization with the beam signal measured in the Target Chamber with the Fast Faraday Cup on a later pulse to establish the beam current and power impinging on the target plane. This shows that for 330 kV diode extraction voltage the beam current is 35.8 mA with a slight 0.7 mA/μs droop associated with the droop of the Marx voltage over this period. Thus, the beam is delivering 11.8 mJ/μs beam power over the flattop region. Several microseconds of this intensity has been used to commission new diagnostics that measure the transient temperature increase of thin foil targets.

In the induction bunching module (IBM) radial electric fields are generated in the gap across which the IBM voltage is applied that include a net radial defocusing effect on the bunching beam. Following an analysis of this effect [15], it was determined that tuning the initial beam envelope to compensate for the defocusing of the IBM enabled simultaneous transverse focusing and axial compression [16], as shown below.

For a tune that optimizes the compressed beam fluence, the variation of spot radius with beam current (and power) is shown in Fig 5. Here the changes to the spot radius and transverse distribution are evident in this time scan across the compression peak. The peak beam current is 1.5 A, and the peak fluence is ≈1 mJ/cm^2/ns At peak compression, 50% of the beam flux is within a radius of 1.5 mm. Higher peak beam current (2.6 A) was reported in [16], and the cause of the difference between the measurements is still being investigated. Topics under study include: diagnostic differences (new vs old fast Faraday cup), detector alignment, IBM waveform fidelity, and plasma density differences. Meanwhile, all the scintillator data and the fast Faraday cup data consistently show the bunch duration is ≈2.5 ns.

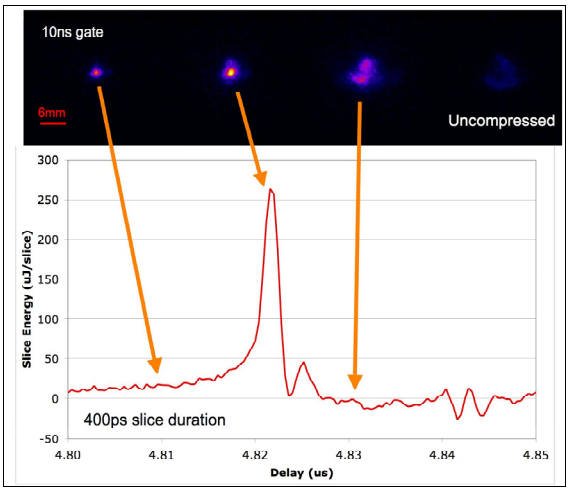

Figure 5: Time-dependent transverse beam distributions demonstrating the simultaneous transverse focusing at the time of peak compression. The peak is ≈2.5 ns FWHM.

Meanwhile, the spot size in these recent measurements is ≈2.1x smaller compared to ref. [16]. Two significant

changes to the experiment are the transverse focusing supplied by the 8-Tesla final focusing solenoid and the modifications to the FCAPS described above. This is a significant improvement, though not as great as expected from PIC simulations assuming ideal neutralization. PIC simulations using the experimentally constrained plasma density distribution are underway which may lead to plasma injection modifications.

FURTHER IMPROVEMENTS

Since mirroring of the plasma injected from outside the solenoid can limit the plasma density in the bore of the focusing element, we are exploring modification of the magnetic field topology near the target plane to allow more efficient plasma transport to the highest field region of solenoid while maintaining high plasma density near the target and in the fringe field of the solenoid. Modeling of plasma flow with auxiliary coils is underway. Also, more compact plasma sources are possible and are being designed. Smaller sources can be placed closer to the target plane, mitigating the limitations of cross-field plasma transport.

We have recently constructed a new IBM with 20 induction core units, or nearly twice the volt-seconds available compared to the present setup. The experiment design question is whether the increased capability should be used, for example, to impart a higher velocity tilt, $\Delta = \delta v/v_o$, (higher peak voltage), or keeping it unchanged for a shallower slope of the tilt and a correspondingly longer drift compression length. The trade-off is between a shorter bunch duration (and greater chromatic aberration), or a smaller spot size and longer pulse duration. The energy deposition on the target scales as [1]:

$$E \underset{\sim}{\propto} \frac{e\phi I\tau}{\varepsilon f\Delta} \qquad (3)$$

where $e\phi$ is the ion kinetic energy, I is the beam current before compression, τ is the initial pulse duration before compression, ε is the un-normalized transverse emittance of the beam. This is based on assuming that all slices of the beam enter the solenoid at radius r_0 independent of velocity. Chromatic aberrations' influence on the spot radius scales as $(\Delta)^{1/2}$. Thus, keeping the focal length approximately the same in the experiment (attractive because of the simplicity) by increasing Δ and τ to use the additional volt seconds cancel in the above scaling. Conversely, doubling the τ, keeping Δ fixed, and doubling the drift compression distance (distance from the IBM gap to the target plane) approximately doubles E, and doubles the compressed pulse duration under the assumption of conservation of longitudinal emittance. We tested these scaling arguments with a series of analytic approximations and LSP simulations [1]. It is advantageous to double the drift compression distance by (+1.44 m) via extension of the FEPS. The expected fluence on the target (≈0.5 J/cm^2) is satisfactory for initial warm dense matter target experiments.

Time-dependent focusing to compensate for the large and limiting chromatic aberration in the bunched beam is desirable. Presently, chromatic aberrations increase the rms focal spot size by about a factor of two. Applying the correction over a longer timescale is technically easier to achieve, thus the correction should be applied near the IBM. A first examination of requirements for a time-dependent lens indicates that a pulsed electric einzel lens or quadrupole doublet with relatively low potentials (10-20 kV) meet the requirements. A quadrupole triplet would allow correction of non-axisymmetric rms-envelope parameters at injection to the bunching module to be brought to an axisymmetric distribution at the focal plane. These will be studied in numerical simulations.

ACKNOWLEDGEMENTS

M. Dickinson, W. Greenway, T. Katayanagi, C. Lee and C. Rogers provided outstanding technical support.

REFERENCES

[1] J.J. Barnard et al., these proceedings.

[2] S.A. MacLaren *et al.*, Phys. Plasmas, Vol. 9, No. 5, (2002), http://link.aip.org/link/?PHPAEN/9/1712/1

[3] D. V. Rose, *et al.*, PAC'01, Chicago, June 2001, RPAH068 http://accelconf.web.cern.ch/AccelConf/p01/PAPERS/RPAH068.PDF

[4] P.K. Roy et al. Nuc. Inst. & Meth. A 544 (2005) 225-235. E. Henestroza et al., PRST-AB 7, 083501 (2004), http://prst-ab.aps.org/abstract/PRSTAB/v7/i8/e083501

[5] P.C. Efthimion et al., PAC07, http://accelconf.web.cern.ch/AccelConf/p07/PAPERS/THPAS082.PDF

[6] P.K. Roy et al., Phys. Rev. Lett. 95, 234801 (2005).

[7] D.R. Welch, D.V. Rose, B.V. Oliver, R.E. Clark, Nuc. Instr. and Meth. A 464, (2001) 134.

[8] A.B. Sefkow and R.C. Davidson, PRST-AB 10, 100101 (2007), and references therein. http://prst-ab.aps.org/abstract/PRSTAB/v10/i10/e100101

[9] F.M. Bieniosek et al., To be published in Nucl. Inst. & Meth. A (NIM-A).

[10] A.B. Sefkow et al., PRST-AB 9, 052801(2006) http://prst-ab.aps.org/pdf/PRSTAB/v9/i5/e052801

[11] F.M. Bieniosek, et al., HIF'04, Nucl. Inst. & Meth. A (2005), 544, 268-276.

[12] F.M. Bieniosek and M. Leitner, PAC'07, Albuquerque, June 2007 FRPMS018, http://cern.ch/AccelConf/p07/PAPERS/FRPMS018.PDF

[13] J.E. Coleman, *Intense Ion Beams for Warm Dense Matter Physics,* PhD Thesis, Univ. of California at Berkeley (2008).

[14] P.K. Roy et al., To be published in Nuclear Instruments and Methods in Physics Research, Section A (NIM-A).

[15] D.R. Welch et al., Nucl. Instrum. Meth. Phys. Res. A 577, 231 (2007).

[16] J.E. Coleman; et al., PAC'07, Albuquerque, June 2007, THPAS004. http://accelconf.web.cern.ch/accelconf/p07/PAPERS/THPAS004.PDF